AJNR

Magnetization Transfer Ratio of White Matter Hyperintensities in Subcortical Ischemic Vascular Dementia

Jody L. Tanabe, Frank Ezekiel, William J. Jagust, Bruce R. Reed, David Norman, Norbert Schuff, Michael W. Weiner, Helena Chui and George Fein

This information is current as of May 15, 2025.

Magnetization Transfer Ratio of White Matter Hyperintensities in Subcortical Ischemic Vascular Dementia

Jody L. Tanabe, Frank Ezekiel, William J. Jagust, Bruce R. Reed, David Norman, Norbert Schuff, Michael W. Weiner, Helena Chui, and George Fein

BACKGROUND AND PURPOSE: **In subjects with subcortical ischemic vascular dementia (SIVD), tissue vacuolization, myelin pallor, and demyelination have been found on pathologic examination of white matter signal hyperintensities (WMSH). Magnetization transfer ratio (MTR) values provide a potential measure of compromised white matter integrity. The purpose of this study was to determine if there were differences in MTR of WMSH between subjects with SIVD and cognitively normal healthy control subjects.**

METHODS: **Fifteen subjects with SIVD and 16 control subjects of comparable age and sex were studied. MTR images were coregistered to MR images segmented into tissue classes (gray matter, white matter, CSF, WMSH, and lacunar infarcts). MTR of WMSH was compared across groups and examined by WMSH location, size, and total burden.**

RESULTS: **WMSH burden was greater in SIVD patients than in control subjects (2.4% vs 0.67%). MTR of WMSH did not differ between groups, but MTR of periventricular WMSH was lower in SIVD patients than in control subjects (37.6% vs 39.4%). Even after accounting for covariant effects of lesion burden, there was still a trend toward reduced periventricular WMSH MTR in the group with dementia. There was no correlation between WMSH MTR and WMSH lesion size.**

CONCLUSION: **These findings are consistent with observations that pathologic changes in vascular dementia are most severe in the periventricular white matter and suggest that insight into the pathophysiology of SIVD might be gleaned from studies of the periventricular region.**

Vascular dementia is the second most common cause of dementia in the United States. The patient must meet six criteria for a positive diagnosis (1);

among them the presence of cerebrovascular lesions (subcortical, cortical, and lacunar infarcts, and white matter signal hyperintensities [WMSH]) on neuroimaging studies and a temporal relationship between those lesions and intellectual decline (1, 2). Thus, neuroimaging plays a crucial role in the work-up of vascular dementia. WMSH lesions are common in normal aging (3–7), however, and are strongly associated with risk factors for vascular disease (3, 6). Furthermore, there is no simple relationship between WMSH and cognition (8–12), so it is important to identify an independent neuroimaging marker for vascular dementia. WMSH lesions are characterized by variable degrees of gliosis, vacuolization, myelin pallor, and demyelination (5, 13–15). There may be differences in the extent, location, or nature of white matter disease in subjects with vascular dementia as compared with normal aging or Alzheimer dementia (16, 17). T2-weighted MR imaging is sensitive, but not specific, for these various disorders. An MR technique potentially more sensitive (18, 19) and specific (20–22) for detecting white matter demyelination is that of magnetization transfer ratio (MTR) measurements (23).

We tested the hypothesis that MTR of WMSH is lower in subjects with subcortical ischemic vascular dementia (SIVD) than in elderly healthy control subjects. We also investigated the effect of WMSH lesion location, size, and burden on MTR of WMSH. This was accomplished by using a previously described semiautomated technique for examining tissue-specific MTR (24).

Methods

Subjects

Subjects were recruited from a university dementia clinic and from Department of Veterans Affairs hospitals and clinics. Inclusionary criteria were the presence of at least one subcortical lacunar infarct identified on MR images and a clinical dementia rating (CDR) of 1 (0 = cognitively normal, 0.5 = cognitively impaired, 1 = demented, 2 = severely demented). For all subjects, we obtained a general medical history, physical examination, neurologic examination, serum chemistry, blood count, thyroid function tests, and B_{12} assessment. In addition, comprehensive neuropsychological testing was performed in all subjects to assess general cognitive function, language, visuospatial ability, executive function, memory, and attention. General cognitive function was assessed with the mini-mental status examination (MMSE).

Subjects were excluded if they met any of the following criteria: older than 55 years of age, non-English speaking, severe dementia (CDR > 2), alcohol or substance abuse, severe head trauma, severe medical illness, neurologic or psychiatric disorders, medications that affect cognitive function, abnormal B_{12} or thyroid metabolism, cortical infarction, or structural brain disease other than lacunar infarcts and WMSH.

The protocol was approved by all institutional review board committees, and all subjects or their legal guardians gave written informed consent before participating in the study.

MR Acquisition

All studies were performed on a 1.5-T MR system using a head coil with quadrature detection. The brain imaging protocol was as follows: 1) proton density— and T2-weighted spin-echo axial images (2500/20,80/1 [TR/TE/excitations]), 3-mm-thick sections with no gap, and 0.94×0.94 mm² in-plane resolution; 2) T1-weighted 3D magnetization prepared rapid gradient-echo coronal images (10/4/1), 1×1 mm² in-plane resolution, and 1.4-mm-thick partitions; and 3) magnetization transfer ratio images with a 3D axial fast gradient-echo sequence that was intermediate between T1- and proton density–weighted (55/6/1), a flip angle of 10°, 4-mm-thick partitions, and 0.94×0.94 mm² in-plane resolution. Although the optimal sequence would be proton density–weighted, a shorter TR was chosen (thus adding some T1 weighting) to reduce scan acquisition time. A 3D data set was obtained without and with magnetization transfer. Saturation was achieved by applying a 7.8-millisecond gaussian-shaped saturation pulse with a magnitude of 9 μT (B_1) 1500 Hz downfield of the narrow water resonance. The specific absorption rate was below the FDA limits for all subjects.

Image Analysis

The procedure for image analysis is an extension of previous work performed in this laboratory (24). To summarize, T1- and T2-weighted images were used for segmentation as follows: the skull was stripped from the images, the 3D T1-weighted images were coregistered to the spin-echo dataset (25), a 3D inhomogeneity filter was applied, and the whole brain was segmented into CSF, white matter, and gray matter, using k-means

cluster analysis (26). This initial, automated process was followed by manual editing on a section-by-section basis to separate cortical from subcortical gray matter, ventricular from sulcal CSF, and to reclassify pixels incorrectly classified as gray matter as WMSH. Two additional steps in the editing process were then performed. First, lacunar infarcts were manually outlined under the supervision of a neuroradiologist, and second, because it is known that MTR in the compact fibers of the corpus callosum are higher than in other white matter regions, the corpus callosum was excluded from analysis by tracing the smallest rectangular block that enclosed the corpus callosum on the midline sagittal image and extending this block on either side of the midline by 2 cm.

MTR Images

The procedure for calculating MTR images is the same as described in our previous report except that MTR values were computed and analyzed as floating point values (32-bit single precision) to reduce scaling error and rounding error effects.

Combining MTR and Segmentation Data

The MTR datasets were resectiond to match the segmented spin-echo data set and combined with the edited segmentation images. The preceding steps in the analysis are shown graphically in Figure 1A–C.

Analysis of Periventricular WMSH

WMSH of the periventricular region was analyzed separately from the rest of WMSH in the region of growth within the ventricular space. A within-section two-pixel region growth of the ventricular space produced an image of the ventricle enlarged by approximately 3 mm on each side. The overlap between the WMSH regions and this enlarged ventricular region was defined as periventricular WMSH (Fig 1D). We excluded all pixels of a tissue category that were immediately adjacent to a pixel of another category to reduce partial volume effects for all tissue categories (including periventricular WMSH).

Statistical Analysis

The percentage of tissue classes (normalized to total intracranial vault), MTR of white matter, cortical gray matter, and total and periventricular WMSH were the dependent variables. Tissue contributions were compared using a two-tailed t-test assuming unequal variance. For MTR analysis, median values within subjects were analyzed as a more robust estimate of central tendency. Initial hypothesis testing of MTR data used analysis of variance (ANOVA), and subsequent testing used analysis of covariance (ANCOVA) with the percentage of WMSH and the MTR of periventricular WMSH as covariates. Correlation analyses were performed using Pearson product moment correlations.

Results

Demographics

There was no difference in age or sex between the groups. MMSE scores and years of education were significantly lower in patients with SIVD as compared with control subjects (Table 1).

MTR

MTR of total WMSH was lower than MTR of normal white matter in both SIVD patients and control subjects. MTR of total WMSH did not dif-
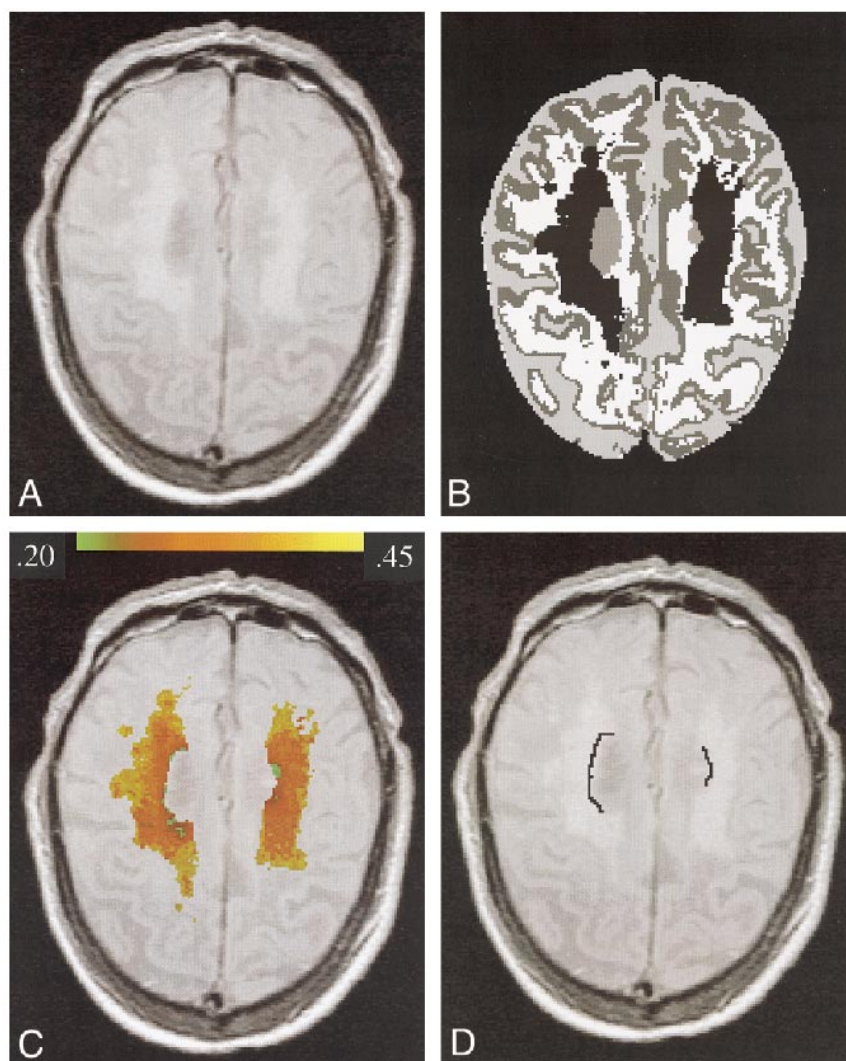
FIG 1. *A–C, A,* Proton density–weighted section from a subject with extensive WMSH; *B,* corresponding segmentation section showing different tissue classes (WMSH in *black*); *C,* color-coded map of MTR of WMSH (*green* corresponds to lowest MTR and *yellow* to highest MTR, shown in the color bar); and *D,* a sample of periventricular WMSH (*black line,* defined as those pixels representing the overlap between WMSH and a two-pixel region grown of ventricular space but excluding all partial volumed pixels (see Methods for details).

TABLE 1: Demographic data for healthy control subjects and subjects with subcortical ischemic vascular dementia (SIVD)

	Control Subjects (n = 16)	SIVD Subjects (n = 15)
Female/male	7/9	6/9
Age (y)	79.9 ± 5.1	79.5 ± 5.6
(range)	(74–88)	(72–91)
Education (y)	16.9 ± 2.8	11.9 ± 3.8*
MMSE	29.2 ± .9	21.0 ± 4.3*

Note.—Values are mean ± 1 SD. MMSE indicates score on minimental status examination.

* $P < .001$

FIG 2. MTR of periventricular and nonperiventricular WMSH for control subjects and patients with SIVD. Values are mean ± 1 SD; *P* values are before correction of the percentage of WMSH.

fer between the groups. On the other hand, MTR of periventricular WMSH was lower in SIVD patients than in control subjects ($P < .01$) and, in both groups, exhibited a tendency to be lower than MTR of nonperiventricular WMSH (Fig 2; $P < .05$ for SIVD patients, $P < .14$ for control subjects) (Table 2). Lower MTR values in the periventricular area can be seen in Figure 1. MTR of cortical gray matter or normal white matter did not differ between SIVD patients and control subjects (Table 2).
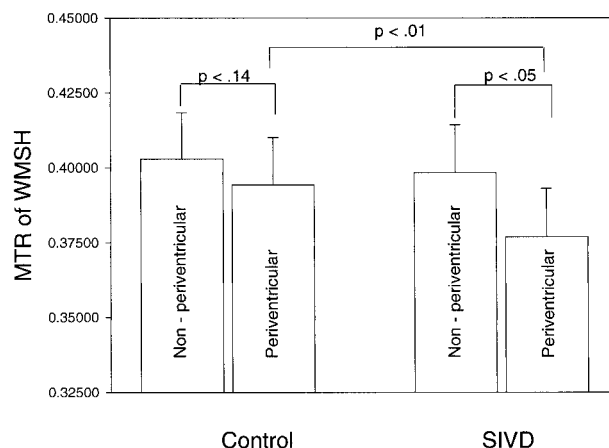
Tissue Segmentation

There was significantly more WMSH ($P < .001$) and larger ventricular volume ($P < .005$) in patients with SIVD than in control subjects (Table 3).

TABLE 2: Magnetization transfer ratio (MTR) of various tissue classes in healthy control subjects and subjects with subcortical ischemic vascular dementia (SIVD)

	Control Subjects (n = 16)	SIVD Subjects (n = 15)
MTR of gray matter	.410	.403
MTR of white matter	.454	.451
MTR of WMSH		
Total lesion load	.403	.395
Periventricular	.394	.376*†
Nonperiventricular	.403	.398

Note.—Values are median. MTR indicates magnetization transfer ratio; WMSH, white matter signal hyperintensities.

* $P < .01$; control vs SIVD subjects before correcting for percentage of WMSH; $P < .08$, after correcting for percentage of WMSH.

† $P < .05$, *t*-test, periventricular vs nonperiventricular WMSH in SIVD patients.

TABLE 3: Tissue contribution in healthy control subjects and subjects with subcortical ischemic vascular dementia (SIVD)

	Control Subjects (n = 16)	SIVD Subjects (n = 15)
Cortical gray matter	37.98 ± 2.23	34.83 ± 2.44
White matter (including WMSH)	34.89 ± 2.25	33.65 ± 2.61
WMSH	0.67 ± 0.64	2.40 ± 1.40*
Ventricular CSF	4.48 ± 1.90	7.68 ± 2.00†
Sulcal CSF	21.48 ± 3.13	22.67 ± 2.63
Lacune	· · ·	.05 ± .07

Note.—Values are percentage of intracranial volume, mean ± 1 SD. WMSH indicates white matter signal hyperintensities.

* $P < .001$, *t*-test, uncorrected for multiple comparisons.

† $P < .005$, *t*-test, uncorrected for multiple comparisons.

The remaining tissue categories showed no significant group difference.

For MTR of periventricular WMSH (dependent variable), there was no interaction between group and WMSH lesion burden (ie, the correlation between WMSH lesion burden and periventricular WMSH MTR behaved similarly for SIVD and control subjects). ANCOVA showed that, after accounting for covariant effects of lesion burden, there was still a trend toward reduced periventricular WMSH MTR in the group with dementia ($P < .08$) (Fig 3).

To determine whether the size of individual WMSH lesions affected the MTR, we analyzed individual lesions for each subject and found no correlation between lesion size and corresponding MTR of that lesion (Fig 4). There was also no correlation between MTR of WMSH and ventricular volume and no difference in the histogram distribution of MTR of WMSH.

We also tested for the possibility that reductions in MTR of periventricular WMSH were an artifact caused by partial volume effects, differences in the abilities of SIVD patients and control subjects to remain motionless during a study, or both. To this end, we examined the MTR of periventricular nor-
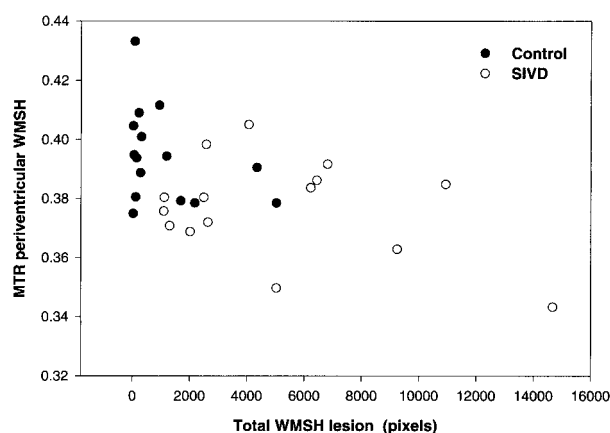

FIG 3. The effect of group and percentage of WMSH on the MTR of periventricular WMSH. Control subjects indicated by *filled circles,* SIVD patients by *open circles.*
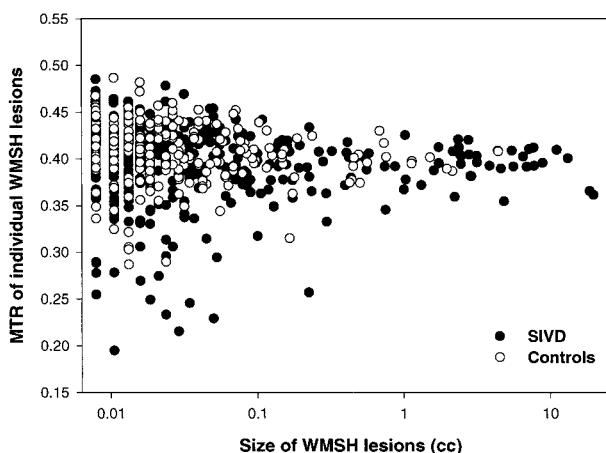

FIG 4. Plot showing no correlation between lesion size and MTR of that lesion for either control subjects or patients with SIVD. Control subjects indicated by *filled circles,* SIVD patients by *open circles.*

mal-appearing white matter and found no differences between MTR of normal-appearing periventricular white matter and other normal-appearing nonperiventricular white matter, either in SIVD or control subjects.

There was no correlation between MMSE score and tissue segmentation or MTR measures.

Discussion

Neuroimaging plays a crucial role in the diagnosis of vascular dementia; the imaging findings consist of cortical infarcts, infarcts in strategic locations, or subcortical infarcts (1–2). Subcortical infarcts in white matter are associated with leukoaraiosis (hypodensity on CT scans or WMSH on MR images). It is well known, however, that WMSH are common in older patients without dementia (4–6, 11, 15), especially if they have risk factors for vascular disease (3, 6, 27). Therefore, it is important to identify markers for vascular dementia independent of and more specific than the

presence of WMSH alone. MTR is an MR technique potentially sensitive and specific for demyelination, and, since demyelination is an important pathologic feature in SIVD (16, 28), we wanted to determine whether MTR could be useful in the work-up of vascular dementia. We found that, compared with cognitively normal elderly control subjects, subjects with SIVD had a greater WMSH burden, no difference in the MTR of the total WMSH burden, but lower MTR of periventricular WMSH.

Our findings are consistent with the observation that among the white matter regions in the brain, the periventricular area tends to be most affected in vascular dementia (16, 17). Erkinjutti et al (16) found that myelin loss in the periventricular area was more severe in patients with vascular dementia as compared with those with Alzheimer dementia. Ishii et al (17) mapped the location, size, and number of lacunar infarcts in 30 necropsy cases of vascular dementia and found the highest density and frequency of lacunar infarcts in the periventricular frontal lobe and caudate head. Furthermore, studies with positron emission tomography suggest that periventricular WMSH may disrupt connections to the frontal lobe that are important in the development of cognitive decline in vascular dementia (29). The pathologic findings in WMSH in the periventricular region may be distinct from nonperiventricular WMSH. Fazekas et al (15) found areas of demyelination and subependymal gliosis corresponding to periventricular WMSH, while ischemic tissue damage corresponded to confluent deep WMSH. Moody et al (30) were the first to describe periventricular venous collagenosis in brain autopsy specimens from neurologically normal patients. Thus, our results are consistent with the idea that pathologic lesions in the periventricular region are different from that in deep WMSH and, moreover, are accentuated in patients with SIVD.

To determine whether MTR measures are any better than indexes of T1, T2, or proton density, we performed additional analyses comparing T1-, T2-, or proton density–weighted pixel intensities (after scaling each subject's data to the median intensity of ventricular CSF). None of these standard imaging measurements resulted in even a weak trend toward differences in MTR of WMSH or periventricular WMSH between SIVD and control subjects. Thus, MTR appears to be more sensitive than conventional MR measurements.

It is less clear why we did not find reduced MTR for the total volume of WMSH. Significant myelin loss observed in subjects with vascular dementia (16, 28, 31) should be associated with lower MTR measurements. While MTR of periventricular WMSH was lower in SIVD subjects, neither total WMSH nor normal-appearing white matter showed group differences. There are several explanations. First, our findings may reflect more demyelination around the ventricles as compared with deep white matter, indicating that the majority of the WMSH burden does not represent demyelination. Second, the reduced MTR may reflect microscopic lacunar infarcts around the ventricles, too small to be resolved as discrete lacunae but large enough to disrupt saturation effects. Finally, the pathologic structure of WMSH in vascular dementia is incompletely understood and is heterogeneous, at best. The entity of Binswanger disease (subcortical arteriosclerotic encephalopathy) comes to mind (31). Considered a subtype of vascular dementia, Binswanger disease is associated with extensive white matter subcortical infarction (1), but Revesz et al (31) have emphasized that it is not a demyelinating process. Though it is rare, we cannot say for certain whether some of our SIVD patients have Binswanger disease.

Our finding of a greater WMSH burden in SIVD patients as compared with control subjects is consistent with other studies, including findings in more mild forms of cognitive performance (6–8). It is important to bear in mind that no simple relationship between lesion load and dementia exists; thus, there is no consensus on the clinical significance of WMSH.

We found no correlation between WMSH lesion size and the MTR of that lesion (Fig 4). Differences in the histopathologic findings between large (>10 mm) and small white matter lesions has been reported (14). Gliosis and vacuolization characterized large white matter lesions, while dilated perivascular spaces characterized the small lesions. Since perivascular spaces are filled with CSF, we might expect lower MTR in the smaller lesions, but found no evidence of this.

Finally, we investigated whether the distribution of WMSH MTR measurements would be biased toward lower values in SIVD patients; that is, that SIVD would have a heavier "left tail" (24). Others have found a similar analysis to be useful for evaluating MTR of multiple sclerosis lesions (32). We found no difference in the left tail distribution of WMSH MTR in SIVD patients and control subjects.

There are several limitations to this study. The first is the relatively small number of subjects in each group. We used rigorous criteria to diagnose SIVD in an attempt to reduce variability in the populations. As a result, our subjects are well characterized, but small in number. Second, partial volume averaging of different tissue classes could be a problem. Nonetheless, several steps (region growing, shrinking, and pixel exclusion) were taken to reduce partial volume averaging as much as possible. The third limitation is that we do not yet have pathologic confirmation for the diagnosis of SIVD. These data are forthcoming, because the subjects will be followed to autopsy.

Conclusion

Vascular dementia is a heterogeneous clinical entity for which several subtypes exist. We reduced

this heterogeneity by studying well-characterized demented subjects with lacunar infarcts and WMSH. We found that MTR of WMSH was not different in subjects with SIVD as compared with the control group, but MTR of periventricular WMSH was lower in the SIVD subjects. Our findings are consistent with observations that, in vascular dementia, pathologic changes (demyelination, vacuolization, and lacunar infarcts) are most severe in the periventricular region. Our results suggest that, while the clinical usefulness of MTR is limited in regard to the diagnosis of SIVD, further insight into the pathophysiology of vascular dementia may be found by neuropathologic investigation of the periventricular region.

References

1. Loeb C, Meyer JS. **Vascular dementia: still a debatable entity?** *J Neurol Sci* 1996;143:31–40
2. Chui HC, Victoroff JI, Margolin D, Jagnot N, Shankle R, Katzman R. **Criteria for the diagnosis of ischemic vascular dementia.** *Neurology* 1992;42:473–480
3. Breteler MMB, van Swieten JC, Bots ML, et al. **Cerebral white matter lesions, vascular risk factors, and cognitive function in a population-based study: the Rotterdam study.** *Neurology* 1994;44:1246–1252
4. Drayer B. **Imaging of the aging brain, 1: normal findings.** *Radiology* 1988;166:785–796
5. Braffman BH, Zimmerman RA, Trojanowski JQ, et al. **Brain MR: pathologic correlation with gross and histopathology, 2: hyperintense white-matter foci in the elderly.** *AJNR Am J Neuroradiol* 1988;9:629–636
6. Longstreth WT, Manolio TA, Arnold A, et al. **Clinical correlates of white matter findings on cranial magnetic resonance imaging of 301 elderly people: the cardiovascular health study.** *Stroke* 1996;27;1274–1282
7. Yliskoski A, Erkinjuntti T, Raininko R, Sarna S, Sulkava R, Tilvis R. **White matter hyperintensities on MRI in the neurologically nondiseased elderly: analysis of cohorts of consecutive subjects aged 55 to 85 years living at home.** *Stroke* 1995;26:1171–1177
8. Breteler MMB, van Amerongen N, van Swieten JC, et al. **Cognitive correlates of ventricular enlargement and cerebral white matter lesions on magnetic resonance imaging: the Rotterdam study.** *Stroke* 1994;25:1109–1115
9. DeReuck J, Decoo D, Strijckmans K, Lemahieu I. **Does the severity of leukoaraiosis contribute to senile dementia?** *Eur Neurol* 1992:32;199–205
10. Bracco L, Campani D, Baratti E, et al. **Relation between MRI features and dementia in cerebrovascular disease patients with leukoaraiosis: a longitudinal study.** *J Neurol Sci* 1993;120:131–136
11. Wahlund L, Basun H, Almkvist O, Andersson-Lundman G, Julin P, Saaf J. **White matter hyperintensities in dementia: does it matter?** *Magn Reson Imaging* 1994;12:387–394
12. Fein G, Van Dyke C, Davenport L, et al. **Preservation of normal cognitive function in elderly subjects with extensive white-matter lesions of long duration.** *Arch Gen Psychiatry* 1990;47:220–223
13. Grafton ST, Sumi SM, Stimac G, Alvord EC, Cheng-Mei S, Nochlin D. **Comparison of postmortem magnetic resonance imaging and neuropathologic findings in cerebral white matter.** *Arch Neurol* 1991;48:293–298
14. Munoz DG, Hastak SM, Harper B, Lee D, Hachinski V. **Pathologic correlates of increased signals of the centrum ovale on magnetic resonance imaging.** *Arch Neurol* 1993:50;492–497
15. Fazekas F, Kleinert R, Offenbacher H, et al. **Pathologic correlates of incidental MRI white matter signal hyperintensities.** *Neurology* 1993;43:1683–1689
16. Erkinjutti T, Benavente O, Elizsziw M, et al. **Diffuse vacuolization (spongiosis) and arteriolosclerosis in the frontal white matter occurs in vascular dementia.** *Arch Neurol* 1996;53: 325–332
17. Ishii N, Nishihara Y, Imamura T. **Why do frontal lobe symptoms predominate in vascular dementia with lacunes?** *Neurology* 1986;36:340–345
18. Fillippi M, Campi A, Dousset V, et al. **A magnetization transfer imaging study of normal-appearing white matter in multiple sclerosis.** *Neurology* 1995;45:478–482
19. Loevner L, Grossman R, Cohen J, Lexa F, Kessler D, Kolson DL. **Microscopic disease in normal appearing white matter on conventional MR images inpatients with multiple sclerosis: assessment with magnetization transfer measurements.** *Radiology* 1995;196:511–515
20. Dousset V, Grossman RI, Ramer KN, et al. **Experimental allergic encephalomyelitis and multiple sclerosis: lesion characterization with magnetization transfer imaging.** *Radiology* 1992;182: 483–491
21. Mehta RC, Pike GB, Enzmann D. **Measure of magnetization transfer in multiple sclerosis demyelinating plaques, white matter ischemic lesions, and edema.** *AJNR Am J Neuroradiol* 1996;17:1051–1055
22. Lexa F, Grossman RI, Rosenquist AC. **MR of wallerian degeneration in the feline visual system: characterization by magnetization transfer rate with histopathologic correlation.** *AJNR Am J Neuroradiol* 1994;15:201–212
23. Grossman RI. **Magnetization transfer in multiple sclerosis.** *Ann Neurol* 1994;36:S97–S99
24. Tanabe J, Ezekiel F, Jagust W, et al. **Volumetric method for evaluating magnetization transfer ratio of tissue categories: application to areas of white matter signal hyperintensity in the elderly.** *Radiology* 1997;204:570–575
25. Woods RP, Cherry SR, Mazziotta JC. **Rapid automated algorithm for aligning and reslicing PET images.** *J Comput Assist Tomogr* 1992;16:620–633
26. SAS Institute. *SAS/SAT User's Guide,* **Release 6.03 ed.** Cary, NC: SAS Institute; 1988
27. Hijdra A, Berbeeten B, Verhulst J. **Relation of leukoaraisosis to lesion type in stroke patients.** *Stroke* 1990:21;890–894
28. Del Ser T, Bermejo F, Portera A, Arredondo JM, Bouras C, Constantinidis J. **Vascular dementia: a clinicopathological study.** *J Neurol Sci* 1990;96:1–17
29. Sultzer DL, Mahler ME, Cummings JL, et al. **Cortical abnormalities associated with subcortical lesions in vascular dementia: clinical and positron emission tomographic findings.** *Arch Neurol* 1995;52:773–780
30. Moody D, Brown WR, Challa VR, Anderson RL. **Periventricular venous collagenosis: association with leukoaraisosis.** *Radiology* 1995;194:469–476
31. Revesz T, Hawkins CP, du Boulay E, Barnard RO, McDonald WI. **Pathological findings correlated with magnetic resonance imaging in subcortical arteriosclerotic encephalopathy (Binswanger's disease).** *J Neurol Neurosurg Psychiatry* 1989:52;1337–1344
32. VanBuchem M, Udupa J, McGowan J, et al. **Global volumetric estimation of disease burden in multiple sclerosis based on magnetization transfer imaging.** *AJNR Am J Neuroradiol* 1997; 18:1287–1290